Hindawi
Advances in Materials Science and Engineering
Volume 2019, Article ID 1684580, 6 pages
https://doi.org/10.1155/2019/1684580

Research Article

Effects of High-Density Pulse Currents on the Solidification Structures of Cu-SiC_p/AZ91D Composites

Xi Hao,[1,2] Weixin Hao,[3] Guihong Geng,[4] Teng Ma,[3] Chen Wang,[1,2] Fuqiang Zhao,[1,2] Hao Song,[1,2] and Yugui Li[1,2,3]

[1]*The Coordinative Innovation Center of Taiyuan Heavy Machinery Equipment, Taiyuan University of Science and Technology, Taiyuan 030024, China*
[2]*Shanxi Provincial Key Laboratory of Metallurgical Equipment Design and Technology, Taiyuan University of Science and Technology, Taiyuan 030024, China*
[3]*School of Materials Science and Engineering, Taiyuan University of Science and Technology, Taiyuan 030024, China*
[4]*School of Materials Science and Engineering, North Minzu University, Yinchuan 750000, China*

Correspondence should be addressed to Weixin Hao; wxhao@vip.sina.com and Yugui Li; liyugui2008@163.com

Received 11 December 2018; Revised 21 February 2019; Accepted 11 March 2019; Published 3 April 2019

Guest Editor: Alena Šišková

In this study, Cu-SiC_p/AZ91D composites were prepared with high-density pulse currents. The wettability between SiC_p and matrix during solidification was improved by coating 0.095-μm thick copper film on the surface of SiC_p. By comparing the composites prepared with/without pulse currents, the solidification structure and its formation mechanism of Cu-SiC_p/AZ91D composites were analyzed under different conditions. The Cu-SiC_p/AZ91D composites prepared without high-density pulse currents were mainly composed of α-Mg, β-$Mg_{17}Al_{12}$, and a small amount of Mg_2Si phases, with coarse grains and uneven structures. Under the action of high-density pulse currents, the structures of Cu-SiC_p/AZ91D composites were transformed into α-Mg and Mg_2Si phases with refined grain, and the homogeneity of the structures was improved significantly.

1. Introduction

Magnesium matrix composites are widely used in aerospace, construction, marine, and mineral processing industries due to their low density, good mechanical properties, and good corrosion resistance [1–3]. However, the performance of traditional magnesium alloys can no longer meet the needs of social development, and people are committed to the preparation of high-performance magnesium alloys. At present, the commonly used preparation methods of magnesium matrix composites include powder metallurgy, stirring casting, in situ synthesis, and melt infiltration methods [4–6]. After treatment, the reinforced particles are evenly distributed, and the properties of alloys are improved. However, these preparation methods require strict pretreatment procedures, high manufacturing costs, and complex operation. As a new technology, the treatment of alloy melt by using high-density pulsed current has attracted the attention of researchers, and some research results have been achieved. Especially under the action of high-density pulsed current, it can effectively inhibit the segregation of the second phase and refine the solidification structure. At the same time, this technology has the characteristics of in situ synthesis technology for some composite materials [7–9].

SiC particles are often used as reinforcing phase for magnesium matrix composites. However, the surface activity of micron and nano-SiC particles is easy to agglomerate, and the wettability of SiC particles is poor [10]. The wettability can generally be improved by increasing the surface energy of the reinforcing phase to lower the surface tension of the melt. Preheat treatment of reinforcing particles, addition of appropriate elements to melt, surface coating, and ultrasonic dispersion can be adopted. Therefore, the modification of the SiC surface is beneficial to

promote the wettability of interface and the uniform distribution of reinforcing particles in the process of liquid casting. At present, the volume fraction of SiC reinforcing phase added by the full liquid stirring casting method is 5 vol.%~10 vol.% [11]. In this paper, a new type of full liquid treatment device under the condition of electric pulse is used. SiC particles coated with copper film are added into the AZ91D matrix as reinforcing phase to improve the wettability of the matrix and reinforcing phase. The Cu-SiC_p/AZ91D composites prepared under different conditions are studied. The microstructures of AZ91D composites and the strengthening mechanism are discussed, which provides a new design concept and method for future research.

2. Experimental

Cu-SiC_p/AZ91D composites contain 10 vol.% Cu-SiC_p, in which a layer of 0.095 μm copper film is deposited on the surface of SiC_p. The mass of Cu is 17.3% of that of Cu-SiC_p. The sample size of AZ91D magnesium alloy is 16 mm × 16 mm × 30 mm. The chemical composition of the AZ91D alloy is shown in Table 1 [12]. The magnesium alloy was used as the matrix in the experiment, and 10 μm SiC particles were chosen as the reinforcer to prepare Cu-SiC_p/AZ91D composites.

Figure 1 shows the schematic diagram of the electric pulse melting device used in this study. The preparation process is described as follows. Firstly, magnesium alloy samples were placed in the boron nitride crucible, and then, SiC_p was placed on the surface of magnesium alloys. The pressure in the vacuum box was pumped to 2×10^{-4} Pa, and then, argon gas was filled to the pressure of 50 kPa. Then turning on the high-frequency induction power supply, the samples were heated to 700°C in the vacuum box, and all the samples were melted in the crucible. Then, the metal melt was heated for 10 min. Finally, the electric pulse was applied to the metal melt for 5 min. The electric pulse treatment process of the metal melt was provided as follows. First, set the pulse width 10 μs, the frequency is 30 Hz, and start the power, then read the required current peak on the oscilloscope by adjusting the voltage, and finally the heating device was closed to start the cooling process in the furnace. When the body was completely solidified, the pulse power supply was turned off.

The structure and composition of the samples were analyzed by SS-550 Shimadzu scanning electron microscope, Phoenix EDAX-2000 energy dispersive spectrometer, and X-ray diffractometer (6000×).

3. Results and Discussion

3.1. XRD Analysis of Solidification Structures. XRD analysis was carried out with the prepared magnesium matrix composites (Figure 2). As shown in Figure 2, the Cu-SiC_p/AZ91D magnesium matrix composites prepared under conventional conditions mainly consist of three phases: α-Mg, β-$Mg_{17}Al_{12}$, and Mg_2Si. The composites prepared under pulse currents mainly consist of two phases: α-Mg and Mg_2Si, and the diffraction peaks of Mg_2Si are enhanced.

Table 1: Chemical composition of AZ91D alloy.

ω (%)					
Cu	Al	Zn	Mn	Si	Mg
0.015	9	0.67	0.25	0.05	Bal.

Note: reproduced from Zhang et al. [12], under the Creative Commons Attribution License/public domain.

3.2. SEM Analysis of Solidification Structures. In order to further analyze the tissue changes, the samples were photographed at a high solution for elemental scanning. The scanning results are listed in Table 2. The XRD spectrum of Figure 2 and Table 2 indicated that the material was composed of α-Mg phase (Spectrogram 1 and Spectrogram 4). The black skeletal dendrite is α-$Mg_{17}Al_{12}$ phase (Spectrogram 2). The new phase Mg_2Si is formed on the dendrite of β-$Mg_{17}Al_{12}$ (Spectrogram 3). The gray-white structure near Mg_2Si is composed of α-Mg and Al_4C_3 as well as less attached Cu (Spectrogram 5).

Figure 3 shows high-resolution SEM photographs of AZ91D magnesium alloy, Cu-SiC_p/AZ91D magnesium matrix composite, and Cu-SiC_p/AZ91D composite in pulsed electric fields. The AZ91D magnesium alloy is mainly composed of gray-black α-Mg and dark-black skeletal eutectic β-$Mg_{17}Al_{12}$ (Figure 3(a)). The phase of β-$Mg_{17}Al_{12}$ grows along the grain boundary. Figures 3(b) and 3(c) show that the hard strengthening phase Mg_2Si grows along the β-phase after adding Cu-SiC_p, and the Mg_2Si phase replaces the β-$Mg_{17}Al_{12}$ phase after applying pulsed electric fields. This is consistent with the bright white structure shown in Figures 4(b) and 4(c), the formation of Mg_2Si diffraction peaks in Figure 2, and the disappearance of $Mg_{17}Al_{12}$ diffraction peaks. The results show that Mg_2Si precipitates as a heterogeneous nucleation point at the grain boundary. SiC and $Mg_{17}Al_{12}$ peaks were not observed in the XRD spectra (Figure 2). It was inferred that the formation of Mg_2Si was ascribed to the reaction of SiC_p and Al [6]:

$$3SiC + 4Al = Al_4C_3 + 3SiC \quad (1)$$

$$Mg + 2Si = Mg_2Si \quad (2)$$

SiC_p in the copper-SiC_p was depleted, and Cu was distributed among the dendrites. Formed Al_4C_3 was dispersed in the vicinity of Mg_2Si [2]. Al_4C_3 was mixed with the matrix α-Mg, thus changing the color from gray to gray-white (red circle in Figure 3(c)), which was consistent with Spectrogram 5 in Table 2. The color change in Figure 3(b) was not obvious because SiC_p was not mixed evenly, and the content of Al_4C_3 was too small. As a heterogeneous nucleation point, Al_4C_3 increased the nucleation rate and refined grains [13, 14].

Copper-SiC_p used in this study could effectively change the wettability between particles and melt, but segregation of copper-SiC_p still occurred, and a large number of copper-SiC_p had not yet reacted with Al in the melt. Dendrites in the structure were mainly composed of β-$Mg_{17}Al_{12}$ and Mg_2Si phases. Al_4C_3 had fewer heterogeneous nucleation points and poor homogeneity, and the grain refinement effect was

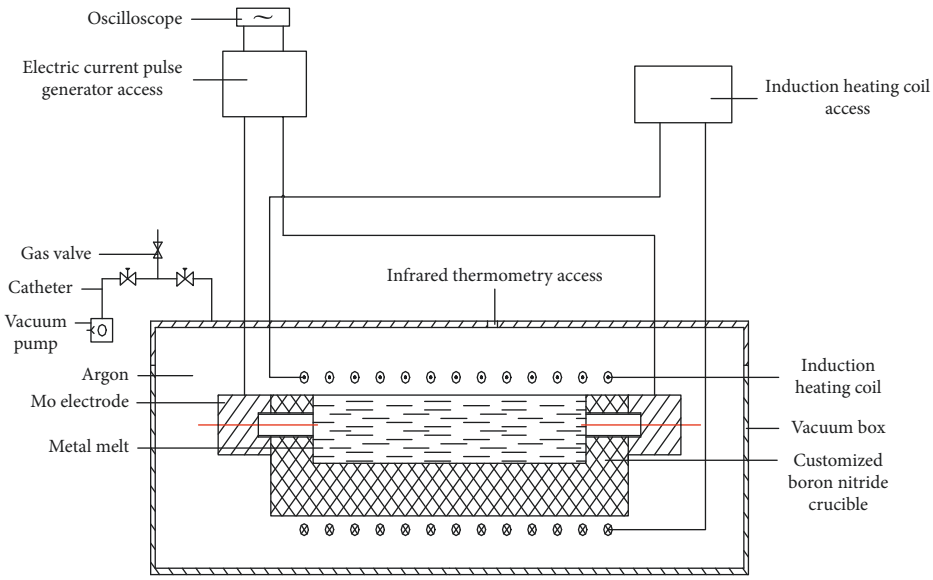

Figure 1: Schematic diagram of the electric pulse melting device.

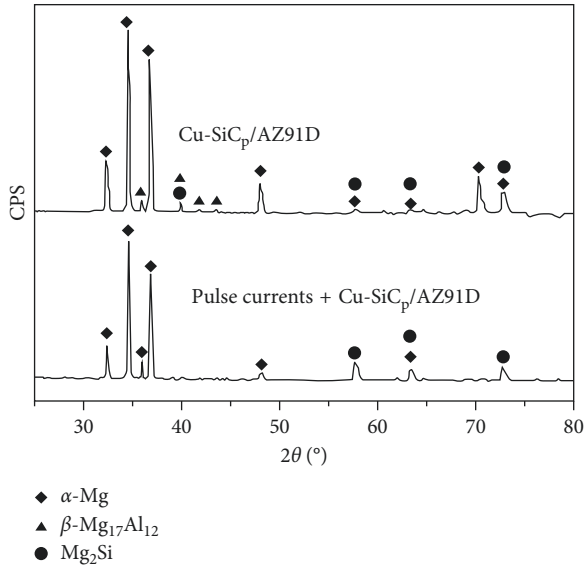

Figure 2: XRD spectrum of Cu-SiC_p/AZ91D magnesium matrix composites.

Table 2: AZ91D and Cu-SiC_p/AZ91D magnesium matrix composite element scanning atomic content table.

Elemental atomic percentage	C	Mg	Al	Si	Zn	Cu
Spectrogram 1	—	90.97	8.27	—	0.76	—
Spectrogram 2	—	60.48	39.52	—		—
Spectrogram 3	—	66.71	—	33.29		—
Spectrogram 4	—	93.78	5.68	—	0.54	—
Spectrogram 5	21.94	51.23	23.84	—	—	2.99

not observed (Figure 3(b)). When high-density pulse currents were applied, the Lorentz force was produced by the metal melt under the action of electric fields [15], and the first cyclotron force of the Lorentz force formed strong convection together with the melt, thus resulting in the decreased temperature gradient, widened two-phase zone in the melt. Therefore, the segregation of Cu-SiC_p was effectively restrained, and Cu-SiC_p was allowed to join the melt and maintained in the uniformly mixing state. Due to the wetting effect and the increase in the contact area, Cu-SiC_p reacted with $Mg_{17}Al_{12}$ sufficiently, thus resulting in phase replacement of β-$Mg_{17}Al_{12}$ phase by the vermicular Mg_2Si (Figure 3(c)). In addition, the formation of a large number of heterogeneous nucleation points Al_4C_3 increased the nucleation rate, promoted heterogeneous nucleation, obtained uniform structures, and further refined the grains [16] (Figure 4(c)).

In the magnesium alloy of AZ91D, α-Mg formed the matrix, and the β-$Mg_{17}Al_{12}$ phase was distributed along the crystal boundary with the large crystal grain. In the Cu-SiC_p/AZ91D composite material obtained under conventional conditions, the tissue was mainly composed of three phases: β-$Mg_{17}Al_{12}$, Mg_2Si, and a small amount of Al_4C_3 phase. Under pulsed electric fields, the composite material showed the uniform structure, and the vermicular Mg_2Si phase replaced the β-$Mg_{17}Al_{12}$ phase. In the vicinity of the Mg_2Si phase, α-Mg was mixed with Al_4C_3 to form the gray-white zone. When a high-density pulse current is applied, the Lorentz force is generated in the melt under the electric field [16], and the melt is strongly convected by the Lorentz force, resulting in a decrease in the temperature gradient inside the melt and a widening of the two-phase region. In this way, the nucleation rate of Cu-SiC_p/AZ91D increased, and crystal grains were refined. After adding Cu-SiC_p particles, the Al_4C_3 phase was not detected because the following hydrolysis reaction occurred in the sampling preparation process [6]:

$$Al_4C_3 + 12H_2O = 4Al(OH)_3 + 3CH_4\uparrow \quad (3)$$

3.3. Refinement Mechanism of Solidification Structures. Figure 3 shows the metallographic pictures of AZ91D magnesium alloy, Cu-SiC_p/AZ91D magnesium matrix

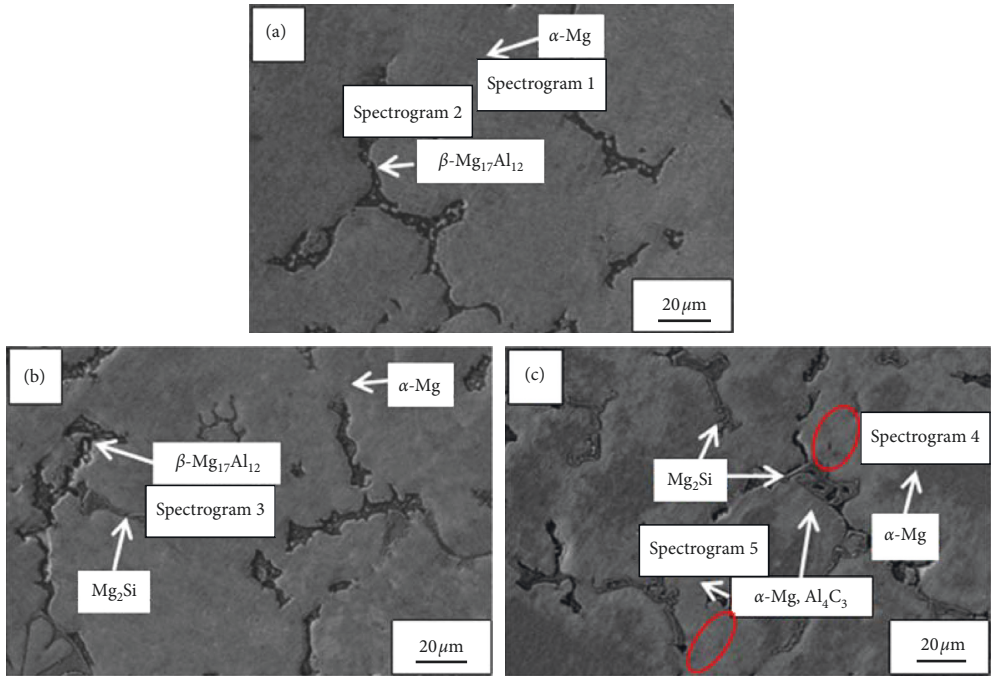

Figure 3: High times SEM of AZ91D magnesium alloy and Cu-SiC_p/AZ91D magnesium matrix composites: (a) AZ91D, (b) Cu-SiC_p/AZ91D, and (c) pulsed electric field+Cu-SiC_p/AZ91D).

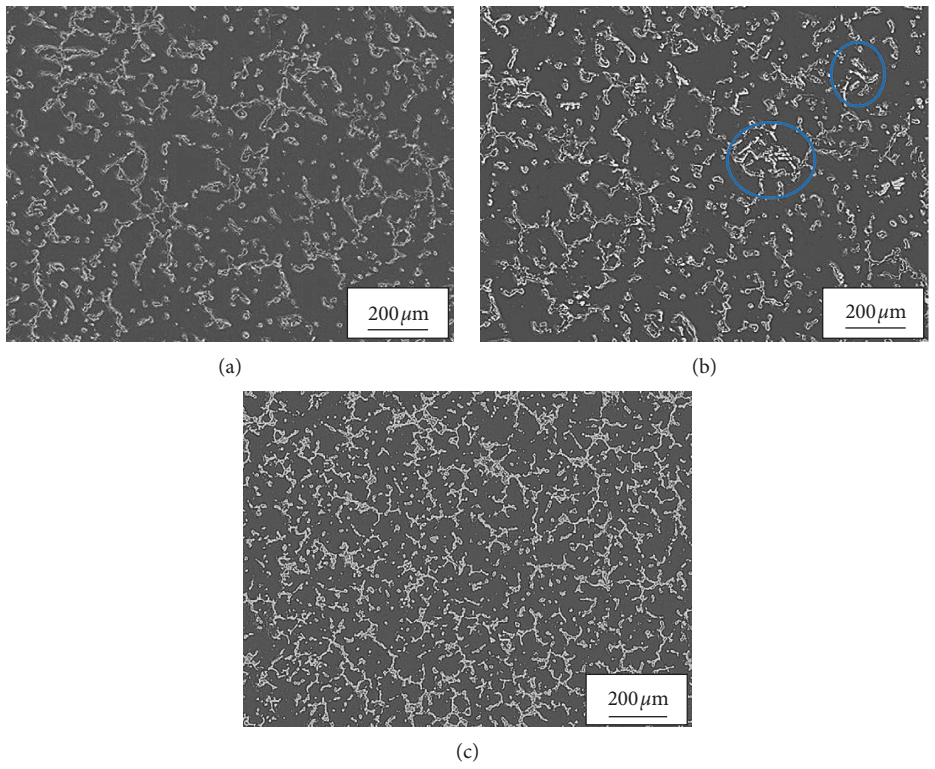

Figure 4: Photos of AZ91D magnesium alloy and Cu-SiC_p/AZ91D magnesium matrix composites: (a) AZ91D, (b) Cu-SiC_p/AZ91D, and (c) pulsed electric field +Cu-SiC_p/AZ91D.

composite, and Cu-SiC_p/AZ91D composite under pulsed electric fields. As shown in Figure 4(a), AZ91D magnesium alloy is composed of black matrix and gray reticulated structure, and its grain size is relatively large. As shown in Figure 3(b), after adding Cu-SiC_p, a little bright white fine structure occurs in the gray-white reticulated structure

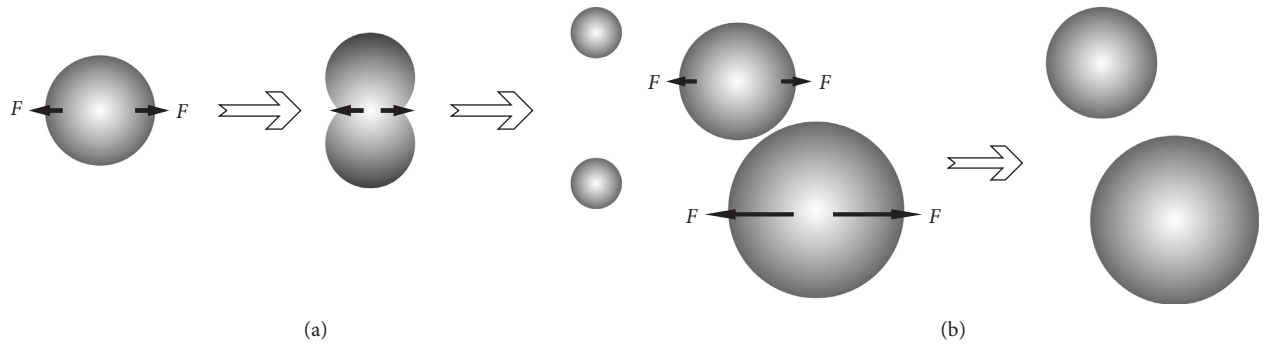

Figure 5: Particle condensation process under the influence of electromagnetic force.

(marked by the blue ellipse), and the grains near the bright white structure are refined Cu-SiC_p that can provide potential nucleation points for the melt, thus increasing the number of fine grains in the composites. The copper-SiC_p particles have the pinning effect on grain boundaries and inhibit the grain growth [17]. As shown in Figure 4(c), after applying pulsed electric fields and adding Cu-SiC_p, all the gray-white reticulated structures become the finer bright white structures with dense dendrites and fine grains.

According to the theory of electromagnetic field dynamics, under the action of pulse currents, the particles and the whole melt are affected by the changing electromagnetic force. This vibration will produce the following effects on the aggregation of particles in the melt. Firstly, the vibration of the electromagnetic force can break coagulated Cu-SiC_p into smaller particles, as shown in Figure 5(a). Secondly, under the action of pulse currents, the SiC particles of different sizes are also affected by inertial force, which results in the relative motion between them. The effect of relative motion also weakens the coagulation effect of Cu-SiC_p, as shown in Figure 5(b). Furthermore, under the action of pulsed electric fields, the undercooling of the alloy melt increases, thus leading to the increase in the viscosity of the alloy melt and weakening the coagulation effect of Cu-SiC_p particles [10, 18].

In order to study the effect of pulse currents on the nucleation rate of alloy melt, the nucleation rate of classical nucleation theory [15] is expressed as follows:

$$N = \frac{nKT}{h}\exp\left(-\frac{16\pi\sigma_{sl}^3 T_m^2}{3L_m^2\Delta T^2 KT}\right)\cdot\ \exp\left(-\frac{\Delta G_A}{KT}\right), \tag{4}$$

where h is the Planck constant; n is the number of atoms per unit volume; K is the Boltzmann constant; T is the absolute temperature; SL is the surface free energy; T_m is the melting point; $\Delta T = (\Delta T_m - T)$ is the undercooling of the alloy melt; L_m is the latent heat of melting; ΔG_A is the liquid atom nucleation barrier. When the axisymmetric current $\vec{j} = j(r)\vec{e_z}$ passes through a cylindrical conductive melt, the magnetic field $\vec{B} = B(r)\vec{e_0}$ is formed. Pulse currents usually affect the undercooling of the alloy melt through the generated Joule heat and electromagnetic force. In addition, when pulse currents are applied during the melt solidification process, more solute atoms are stimulated to break the energy barrier and enter the matrix due to the effect of instantaneous discharge. At the same time, pulse currents enhance the vibration of atoms deviating from the equilibrium position, reduce the energy barrier, and change the nucleation barrier. Therefore, in the original nuclear rate equation (1), $\Delta G_A = (\Delta G_0 + \Delta G_E)$, where G_0 is the thermodynamic barrier for the nucleation without applying an external field and G_E is the thermodynamic barrier for the nucleation after applying an external field. Then, we get

$$\begin{aligned}\Delta G_A &= \left(\Delta G_0 + \Delta G_E\right) = \Delta G_0 + K_1\cdot j_2\cdot\xi_2\cdot V,\\ \xi &= \left(\sigma_0 - \sigma_n\right)\cdot\left(\sigma_n - 2\sigma_0\right)^{-1}.\end{aligned} \tag{5}$$

Among them, K_1 is a parameter related to materials; J is the pulsed current density; σ_0 is the conductivity of disordered dielectrics; σ_n is the conductivity of nuclei; V is the volume of nuclei; and K is the Boltzmann constant. For the crystalline melt, if $\sigma_n > \sigma_0$, then $\xi > 0$. Therefore, it can be concluded that the pulse currents reduce the nucleation barrier in the alloy melt. The effect of pulse currents increases the nucleation rate in the alloy melt, and the increase in the nucleation rate leads to the grain refinement in the alloy melt. When EPT is applied after heat preservation, the pulse currents contact directly with the melt and the nucleation growth stops, thus forming an equiaxed region, which can effectively improve the nucleation rate of liquid metal and semisolid metal and trigger the heterogeneous nucleation mechanism [19]. Fine structures were obtained during the rapid solidification because the increase in the undercooling promoted the nucleation rate. The mechanism of dendrite breakage induced by Loren magnetic force under electric pulse treatment allowed the grain refinement [16, 20].

4. Conclusion

Cu-SiC_p/AZ91D composites prepared without high-density pulse currents mainly consisted of three phases: α-Mg, β-$Mg_{17}Al_{12}$, and Mg_2Si. By applying high-density pulse currents, the structures of Cu-SiC_p/AZ91D composites were transformed into the phases of α-Mg and Mg_2Si.

Cu-SiC_p/AZ91D composites were prepared by different testing methods. The results showed that the Cu-SiC_p/AZ91D composites under high-density pulse currents had uniform structures, and the grains were significantly refined. The nucleation barrier was reduced, and the nucleation rate

was effectively increased by applying high-density pulse currents. Therefore, the fine structure was obtained.

The microstructures of Cu-SiC_p/AZ91D composites were transformed into α-Mg, Al_4C_3 and Mg_2Si phases under the action of high-density pulse currents. Al_4C_3 and Mg_2Si phases as heterogeneous nucleation points increased the nucleation rate of the composites. The Al_4C_3 phase was not detected in the obtained tissues due to the hydrolysis reaction.

Data Availability

The data used to support the findings of this study are available from the corresponding author upon request.

Conflicts of Interest

The authors declare that there are no conflicts of interest regarding the publication of this paper.

Acknowledgments

This work was supported by the National Natural Science Foundation of China (51561001, 51574171, and 51641406), the Natural Science Foundation of Shanxi Province of China (no. 201601D011012), Key Project of Shanxi Key Research and Development Program "Development of Ultra High Strength and Composite Wide and Heavy Plate Large Rolling Equipment" (201703D111003), Shanxi Province Science and Technology Major Project "Research on High Temperature, Corrosion and Wear Resistant Metal Composite Plate/Tube Material Technology": (MC2016-01), and NSFC-Shanxi Coal-Based Low-Carbon Joint Fund Support Project "Research on the Evolution and Performance of Key Materials in Ultra-Supercritical Boilers under Preparation and Service Conditions" (U610256).

References

[1] W.-J. Li, K.-K. Deng, X. Zhang et al., "Microstructures, tensile properties and work hardening behavior of SiC_p/Mg-Zn-Ca composites," *Journal of Alloys and Compounds*, vol. 695, pp. 2215–2223, 2017.

[2] T. J. Chen, X. D. Jiang, Y. Ma, Y. D. Li, and Y. Hao, "Grain refinement of AZ91D magnesium alloy by SiC," *Journal of Alloys and Compounds*, vol. 496, no. 1-2, pp. 218–225, 2010.

[3] S.-Y. Liu, F.-P. Gao, Q.-y. Zhang, X. Zhu, and W.-Z. Li, "Fabrication of carbon nanotubes reinforced AZ91D composites by ultrasonic processing," *Transactions of Nonferrous Metals Society of China*, vol. 20, no. 7, pp. 1222–1227, 2010.

[4] Y. Wu, W. Du, Y. Nie et al., "Research status of particulate reinforced magnesium matrix composite," *Rare Metal Materials and Engineering*, vol. 36, no. 1, pp. 184–188, 2007.

[5] A. Noguchi, I. Ezawa, J. Kaneko, and M. Sugamata, "SiC/Mg-Ce and Mg-Ca alloy composites obtained by spray forming," *Journal of Japan Institute of Light Metals*, vol. 45, no. 2, pp. 64–69, 1995.

[6] T. J. Chen, Y. Ma, W. B. Lv, Y. D. Li, and Y. Hao, "Grain refinement of AM60B magnesium alloy by SiC particles," *Journal of Materials Science*, vol. 45, no. 24, pp. 6732–6738, 2010.

[7] B. T. Zi, K. F. Yao, W. J. Liu, J. Z. Cui, and Q. X. Ba, "Effect of higher density pulsed current on solidification structures of 2024 Al alloy," *Rare Metal Materials and Engineering*, vol. 32, no. 1, pp. 9–12, 2003.

[8] S. Xiaosi, H. Weixin, M. Teng, and G. Geng, "Control of the solidification structure of hypermonotecticCu-40 wt.% Pb alloy melt by pulse currents," *AIP Advances*, vol. 8, no. 10, article 105019, 2018.

[9] M. Teng, H. Weixin, S. Xiaosi, J. Zhang, and G. Geng, "Effects of high-density electric current pulse on the undercooling of Fe-B eutectic alloy melt," *Advances in Materials Science and Engineering*, vol. 2018, Article ID 9721508, 6 pages, 2018.

[10] R. Wu, Q. Li, L. Guo, and Y. Ma, "Fabrication and characterization of bimodal size Al_2O_{3p} reinforced 7075 aluminium matrix composites," *Materials Science*, vol. 23, no. 4, pp. 317–321, 2017.

[11] Q. Yan, S. Li, and X. Wang, "Research progress on SiC_p reinforced AZ91 magnesium matrix composites," *Foundry Technology*, vol. 34, no. 12, pp. 1608–1611, 2013.

[12] L. Zhang, Q. Wang, W. Guo, W. au, W. Li, and H. Ding, "Microstructure and mechanical properties of the carbon nanotubes reinforced AZ91D magnesium matrix composites processed by cyclic extrusion and compression," *Materials Science and Engineering: A*, vol. 689, pp. 427–434, 2017.

[13] E. Yano, Y. Tamura, T. Motegi, and E. Sato, "Effect of pure carbon powder on grain refining of cast magnesium alloy AZ91," *Journal of Japan Institute of Light Metals*, vol. 51, no. 11, pp. 599–603, 2001.

[14] S. Chen, C. Cai, H. Yu et al., "Effect of SiC content on refining efficiency and morphology of AZ91D magnesium alloys," *Special Casting & Nonferrous Alloys*, vol. 33, no. 10, pp. 976–979, 2013.

[15] D. Räbiger, Y. Zhang, V. Galindo, S. Franke, B. Willers, and S. Eckert, "The relevance of melt convection to grain refinement in Al-Si alloys solidified under the impact of electric currents," *Acta Materialia*, vol. 79, pp. 327–338, 2014.

[16] H. Z. Liu, Z. L. Zhao, and L. H. Ma, "Influence of high density pulse electric current on solidified aluminum structure and undercooling degree," *Foundry Technology*, vol. 29, no. 10, pp. 1354–1358, 2008.

[17] Y. Huang, K. U. Kainer, and N. Hort, "Mechanism of grain refinement of Mg-Al alloys by SiC inoculation," *Scripta Materialia*, vol. 64, no. 8, pp. 793–796, 2011.

[18] X. Zhang, S. Wang, and X. Na, "Effect of magnetic field on the solidification of metallic materials," *Journal of Iron and Steel Research*, vol. 26, no. 5, pp. 1–7, 2014.

[19] M. Sugamata, K. Shiina, M. Kubota, and J. Kaneko, "Properties of mechanically alloyed P/M composites of Al–Mg_2Si–oxide systems," *Journal of Alloys and Compounds*, vol. 483, no. 1-2, pp. 350–354, 2009.

[20] M. J. Abou-Khalil, R. J. Gauthier Jr., T. C. Lee et al., "Structures, methods and applications for electrical pulse anneal processes," U.S. Patent 9,881,810, 2018.